Marine Geology 470 (2024) 107255

Contents lists available at ScienceDirect

Marine Geology

journal homepage: www.elsevier.com/locate/margo

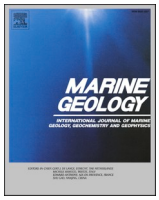

Seismic stratigraphic and sedimentary record of a partial carbonate platform drowning, Queensland Plateau, north-east Australia

Christian Betzler [a,*], Christian Hübscher [b], Sebastian Lindhorst [a], Thomas Lüdmann [a], Carola Hincke [a], Robin J. Beaman [c], Jody M. Webster [d]

[a] Institut für Geologie, Universität Hamburg, Bundesstr. 55, 2046 Hamburg, Germany
[b] Institut für Geophysik, Universität Hamburg, Bundesstr. 55, 2046 Hamburg, Germany
[c] College of Science and Engineering, James Cook University, Cairns 4870, Queensland, Australia
[d] Geocoastal Research Group, School of Geosciences, University of Sydney, Madsen Building (F09), Sydney 2006, NSW, Australia.

ARTICLE INFO

Editor: Michele Rebesco

Keywords:
Carbonate platform
Miocene
Ocean currents

ABSTRACT

Tropical carbonate platforms are edifices built by shallow-water, carbonate-producing organisms. Prolonged suppression or shutdown of tropical shallow-water carbonate factories may result in partial or complete platform demise. Factors triggering the drowning process can relate to rates of accommodation increase exceeding carbonate accumulation and/or the establishment of ecological conditions not favorable for carbonate producers, with increasing water temperatures and high nutrient contents proposed as drivers. More recently, the intensification of ocean circulation and currents has been identified as a major factor in carbonate platform drowning. We tested the latter with seismic reflection and multibeam data collected with RV *Sonne* in 2022 on the Queensland Plateau (north-east Australia) and by correlating these data with ODP Leg 133 sedimentological and biostratigraphic results. The carbonate platforms of the Queensland Plateau underwent a partial drowning between 13.6 and 12.7 Ma. This partial drowning is coeval with the onset of current-driven sedimentation. Relict platforms, which form the core of the presently still active platforms, were established in two steps: After the demise of a spatially expanded platform, a system with smaller, low-relief banks and mounds established. At around 3.7 Ma, there was a turnover and higher relief, flat-topped platforms established. We propose that the geologic history of the Queensland Plateau represents another example of a carbonate platform evolution controlled by ocean currents.

1. Introduction

Ocean currents are a major factor affecting carbonate platform facies and stratigraphy and also contribute to the drowning of carbonate platforms (Isern et al., 2004; John and Mutti, 2005; Bachtel et al., 2010; Eberli et al., 2010; Betzler et al., 2009, 2016, 2023; Ling et al., 2021; Reolid et al., 2020; Thronberens et al., 2022). This is through physical action including erosion and resuspension (Storlazzi et al., 2011), topographically-induced upwelling, and an increase of nutrients potentially displacing hermatypic corals (Hallock and Schlager, 1986), especially on the down-current side of the banks (de Vos et al., 2014), and negative effects on coral larvae settlement (Hata et al., 2017).

Many elements of the modern climate and ocean circulation system were emplaced during the Neogene, such as a permanent Antarctic ice sheet (Sugden et al., 1993) and ephemeral northern hemisphere ice sheets paced by orbital variations (Hays and Imbrie, 1976; Lisiecki and Raymo, 2005). East Antarctica ice sheets triggered a steep global meridional temperature gradient, intensifying atmospheric pressure systems and ocean circulations (Flower and Kennett, 1994; Zachos et al., 2001). Betzler and Eberli (2019) discussed that a current-controlled carbonate platform mode started at this time of Middle to Late Miocene stepwise global cooling (Holbourn et al., 2013) and the onset of modern ocean circulation. In addition to the emergence of current-controlled sedimentation in and around distinct isolated carbonate platforms, partial carbonate platform drowning occurred at the Maldives at ~13 Ma (Betzler et al., 2016) and at the Marion Plateau at ~13.6 Ma (John and Mutti, 2005; Eberli et al., 2010; Bashah et al., 2024), which coincides with this circulation onset. The late Middle Miocene was therefore seen as a major break in global carbonate platform evolution (Betzler and Eberli, 2019).

* Corresponding author.
E-mail address: christian.betzler@uni-hamburg.de (C. Betzler).

https://doi.org/10.1016/j.margeo.2024.107255
Received 14 November 2023; Received in revised form 26 February 2024; Accepted 3 March 2024
Available online 5 March 2024

The goal of this study is to establish whether a similar major break in carbonate platform evolution is also observed on the Queensland Plateau, a partially drowned carbonate platform within Australia's Coral Sea. We use new multichannel seismic data and multibeam data collected during RV *Sonne* Cruise SO292, and sedimentary records from previous Ocean Drilling Program Leg 133 cores, to analyze the evolution and partial drowning of the Queensland Plateau. We demonstrate how ocean current activity controls the carbonate platform evolution.

2. Geological setting

The East Australian carbonate province, which encompasses the Great Barrier Reef, Marion Plateau and Queensland Plateau, has been in the focus of integrated sedimentological, stratigraphic, and palaeoceanographic research during ODP Leg 133 which cored eight sites (Davies et al., 1991; Fig. 1A) as far down as the basement. The Queensland Plateau is detached from the Australian mainland and characterized by about thirty isolated carbonate banks, which are relicts of an older and larger platform (Davies et al., 1989; Fig. 1B). The basement of the Queensland Plateau consists of metasedimentary rocks (Feary et al., 1993) covered by Paleogene *syn*-rift sediments (Mutter, 1977; Taylor and Falvey, 1977). The Eocene-Oligocene boundary is expressed as a regional unconformity capping the rift succession. Carbonate platforms on the Queensland Plateau were established during the middle Eocene (Mutter, 1977; Davies et al., 1991; Betzler et al., 1993), but geometry and distribution of these former neritic carbonates are not clearly imaged in the available data (Fig. 1B).

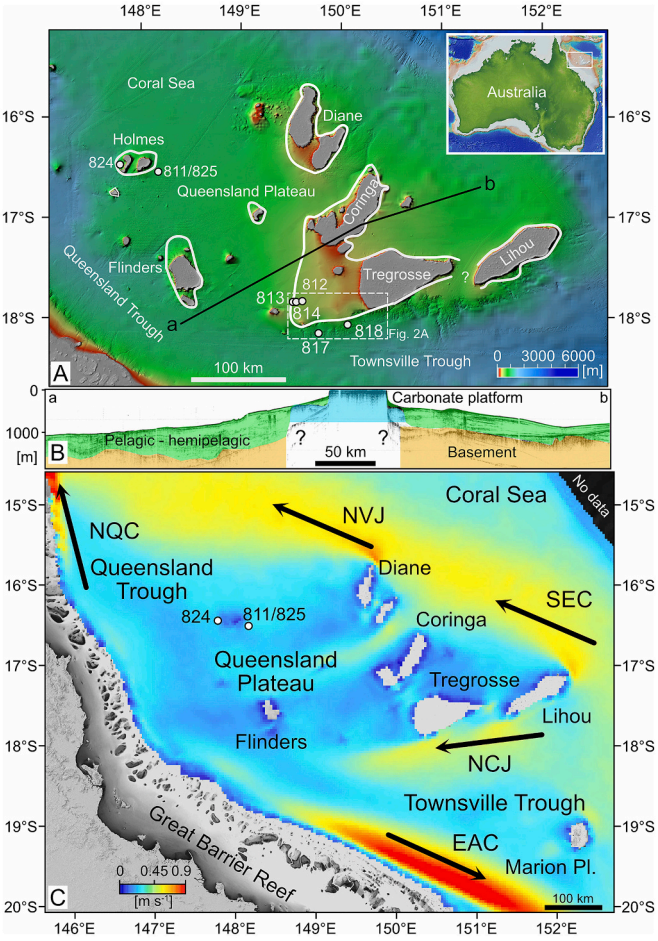

Fig. 1. A: Queensland Plateau with isolated active carbonate banks and ODP sites. The white lines trace the outline of the Miocene shallow-water carbonate platforms after Mutter (1977), Davies et al. (1989) and also based on seismic data acquired during RV *Sonne* cruise 292 in 2022. B: Cross section of the Queensland Plateau with main facies associations and position of the basement using Davies et al. (1989). The section corresponds to seismic line MGD77T acquired during the cruise RC1006 with RV *Robert D. Conrad* in 1966. The line was downloaded from https://www.ngdc.noaa.gov/trackline/request/?surveyIds=RC1006. C: Queensland and Marion Plateau current velocities and directions for the year 2011. Data were extracted via https://extraction.ereefs.aims.gov.au/ (download on August 9, 2023). Currents after Choukroun et al. (2010). Bathymetry from Australian gbr100 data (Beaman, 2010). EAC: East Australian Current; NCJ: North Caledonia Jet; NQC: North Queensland Current; NVJ: North Vanuatu Jet; SEC: South Equatorial Current.

The wind regime over the Queensland Plateau is dominated by the south-easterly trade winds, which as elsewhere are expected to have intensified at 12 Ma (Groeneveld et al., 2017). The general oceanic current pattern in the Queensland Plateau area is controlled by the current system of the South Equatorial Current (SEC; Fig. 1C). The SEC delivers an influx of about 24 Sv, from which 12 Sv exit before reaching the Coral Sea west of the Solomon Islands and Vanuatu (Andrews and Clegg, 1989). When reaching the Queensland Plateau, the SEC comprises the North Vanuatu Jet (NVJ) and the North Caledonian Jet (NCJ), which both show large seasonality (Colberg et al., 2020). The NVJ is a broad, upper thermocline current, whereas the NCJ is narrow and extends to water depths of at least 1500 m (Kessler and Cravatte, 2013). The current system of the SEC undergoes bifurcation east of the Queensland Plateau (around 17–18°S, Brinkman et al., 2002). As a result, the NVJ (about 6 Sv) is directed northwards and forms the North Queensland Current (NQC) or Gulf of Papua western boundary current (Andrews and Clegg, 1989; Kessler and Cravatte, 2013; Colberg et al., 2020). The other branch, originating from the NCJ, (about 6 Sv) turns south and eventually becomes the East Australian Current (EAC), the major western boundary current of the South Pacific gyre, usually observed between 18 and 35°S (Wyrtki, 1962; Church, 1987; Bostock et al., 2006). This south-flowing limb of the SEC current system is the one that is probably linked to the Miocene drowning of the Marion Plateau (Isern et al., 2004; Eberli et al., 2010). The emergent reefs and banks of the Queensland Plateau, which form tower-like structures elevated above the plateau area (Fig. 1), act as obstacles and divert currents flowing over the plateau (Ceccarelli et al., 2013).

The flanks of the Queensland Plateau's emergent reefs and banks appear to be affected by complex currents, including downslope and upwelling systems (Orme, 1977). The seafloor in the passages separating the banks in water depths of 230–240 m is covered by carbonate sands with small- and large-scale ripples observed during spot dives with a submersible (Orme, 1977). Some areas even have no sediment cover and are formed by uneven and eroded surfaces. The surface currents in and around the banks are controlled by the south-easterly trade winds and by the tides, which have amplitudes of up to 1.80 m (Orme, 1977).

Today, the carbonate banks of the Queensland Plateau appear to follow the classical windward-leeward, inner platform facies asymmetry governed by the wind regime: reef rims grow along the windward edge of the banks and protect open lagoons. These lagoons, however, are underfilled with respect to the sediment infill and have water depths of 50–75 m. Pinnacles and knolls representing living coral heads are reported scattered around the seafloor of the open lagoons (Orme, 1977). Although Coringa and Tregrosse banks were and are well located within the trade wind belt, it has been shown that the leeward margin of the platform surrounding these two large banks has stepped back towards the east (Fig. 1), i.e. against the flow, since the Middle Miocene (Mutter, 1977; Taylor and Falvey, 1977; Davies et al., 1989).

The area of this backstepping has been investigated in several studies based on sediment samples from ODP sites 812, 813, and 814 (Supps. 1–6) and some low-resolution seismic lines (Davies et al., 1991). The backstepping of the platform margin was preceded by the replacement of a rimmed platform to what has been interpreted as a carbonate ramp (Betzler, 1997). This change was dated as ~12 Ma and has been interpreted to be a response to a cooling of surface waters, a higher nutrient influx, as well as a changed current and hydrodynamic energy regime

(Isern et al., 1993, 1996; Brachert et al., 1993; Betzler et al., 1995). This would also cause a turnover from a chlorozoan to a heterozoan carbonate factory as described by Brachert et al. (1993) and Betzler et al. (2000). Alternatively, warm surface waters at 11 to 7 Ma suppressing coral reef growth, however, were evoked by Petrick et al. (2023) to cause the profound change of shallow-water carbonate production.

The subsidence rate for the Queensland Plateau has been calculated to 9–11 cm / 1000 yrs. (past 5 Ma), with lower rates before ~3 Ma (Müller et al., 2000). This means that the increase of the subsidence rate started ca. 9–10 million years after the partial platform demise and thus does not appear as a controlling factor of this process.

3. Data and methods

Age assignments of the ODP Leg 133 sites cored on the Queensland Plateau were presented in Davies et al. (1991) and Gartner et al. (1993) based on calcareous nannoplankton and planktonic foraminifer datums as well as large benthic foraminifer occurrences (Betzler and Chaproniere, 1993). In addition, magnetostratigraphic datums (McNeill et al., 1993) were used. Numerical ages for the biostratigraphic datums and the reversals were taken from Raffi et al. (2020) and are summarized in Supplement 1. The lithostratigraphic descriptions of ODP sites 812, 813, and 814 (Davies et al., 1991) were reviewed and standardized, using the core photographs and compositional description. The revised syntheses of the lithostratigraphy are provided in Supplements 2 to 6.

For tracing the onset and the past variations of the current regime, depositional geometries indicative of bottom current activity were observed in high-resolution seismic data. Data were acquired during the RV *Sonne* Cruise SO292, the seismic signals were generated by an array comprising one GI-Gun (true GI-Modus; primary volume of 45 in3) plus one Mini-GI (true GI-Modus; primary volume of 15 in^3), towed 41 m behind the ship's stern at a water depth of ca. 2.5 m. Sources were released equidistantly every 18.75 m at 160 bar. A SureShot trigger system was used to synchronize seismic sources and recording. The streamer was a Hydroscience Technologies SeaMUX 144-channel system with an active length of 600 m and symmetric group interval. The recording length was 4 s, and the sample interval was 1 ms. Data were stored in SEG-Y format. All seismic profiles were processed on board with the 2021 VISTA® desktop seismic data processing software by Schlumberger. The main processing steps comprised bandpass filtering (18/25–350/450 Hz), velocity analysis (every 25–500 CMP), spherical divergence correction, NMO-correction and stack, FD migration, top-mute, data enhancement (white noise removal, fx deco), and scaling. Wavelengths between 10 and 20 m result in a realistic vertical resolution of 5 to 10 m. Processed data were loaded into Petrel software (Schlumberger) for attribute processing, visualization, and interpretation. For the well to seismic ties, the time-depth relationships as presented in the ODP Leg 133 site reports (Davies et al., 1991) were used.

Bathymetric data were acquired at a cruising speed of 5.5 to 8 kn by means of the hull-mounted Kongsberg EM122 multibeam system. The EM122 is a deep-water echosounder with a nominal frequency of 12 kHz and an angular sector coverage of 150° in maximum (typically set to 130–140° to suppress low quality signals from the outer beams). Equidistant beam spacing and dual swath mode were used for all lines. Transmit fans were stabilized for roll, pitch and yaw. Sound-velocity and salinity profiles of the water column were obtained from conductivity-temperature-depth (CTD) probe measurements and by using XSV-02 probes (Lockheed Martin, Sippican Inc.). The similarity of most SO292 sound profiles implies that water-mass stratification was very homogenous throughout the central Queensland Plateau. Ship-mounted sound-velocity (Kongsberg C-Keel) and salinity sensors provided real-time sound velocity and salinity of the near-surface water layer; measures being critical for beam forming. Qimera software (v2.4.8, QPS software) was used for data processing. Data were cleaned manually using the slice- and 3D-editor of Qimera. Surfaces with cell sizes of 30 m were created using the CUBE algorithm and visualized using GlobalMapper (Blue Marble Geographics). Bathymetric data were corrected for astronomic tides using tidal predictions of AusTides software (Australian Hydrographic Office); predictions for stations 57,845 (Magdelaine Cays) and 57,850 (Willis Islet) were used. The multibeam bathymetry data collected by RV *Sonne* cruise SO292 were supplemented by Kongsberg EM302 multibeam data collected RV *Falkor* cruises FK200429 and FK200802 (Siwabessy and Spinoccia, 2022).

Sub-bottom profiles were recorded using the ship's hull-mounted parametric sediment echosounder, Atlas Parasound PS70 (mk2) with the software Parastore (Teledyne RESON GmbH, v3.5.0.3). The desired primary high frequency was 18 kHz, and the secondary low frequency 4 kHz. The PS70 was operated in single pulse mode with a transducer voltage of 100 V, and a transceiver amplification of 30 to 40 dB. Depth of seafloor penetration varies with slope angle, lithology, grain size, and gas load of the sediment; typical sub-seafloor penetration during SO292 was around 10 m on the top of the carbonate banks (water depths around 50–60 m), almost 0 m at steep- and/or lithified parts of the slopes, and 80 to >140 m in the drift sediments surrounding the platforms. Data were converted to SEG-Y using the tool ps32segy (Hanno Keil, University of Bremen, Germany) and processed using the software ReflexW (Sandmeier Software). Processing steps comprised data editing, compensation for trace header delay, gain adjustment (using automatic gain control), and along-profile amplitude normalization. Time-depth conversion of Parasound data was done with a sound velocity of 1500 m s^{-1}.

4. Results and interpretations

4.1. Bathymetry

This study focuses on the area of Tregrosse Bank and the zone west of the bank, where ODP sites 812 to 814 are located (Figs. 1, 2). The western platform edge of Tregrosse Bank lies at water depths of 85 to 90 m (Fig. 2A) and passes into a slope dipping with 10° to 25°. The toe of slope lies at around 200 m. This is followed by a 7 km wide and approximately 10 m deep gentle depression lined by a bulge. Further offbank, the seafloor can be characterized as a plateau, gently dipping (ca. 0.2°) to a water depth of 470 m over a horizontal distance of 50 km (Figs. 2A-C). A 4 km wide zone with a steeper dip (ca. 0.4°) follows down to 550 m. Further west, water depths reaches >1000 m in the Queensland Trough.

Around ODP sites 812 to 814 and east of these sites there are several circular pockmark structures up to 35 m deep and 200 to 450 m wide (Figs. 2B, C). Another seafloor feature is a ca. 30 m high step with a rounded outline lined by a 300 m wide and 20 m deep moat-like depression located 1.5 km southeast of ODP Site 814 (Fig. 2D). Further, located 6 km northeast of Site 814, there is a 500 m wide and up to 20 m deep edge-formed depression.

The southern termination of the plateau is a submarine scarp, which reaches vertical heights of >200 m (Fig. 2D). The scarp forms a sinuous line. The edge of the scarp in general lies at water depths of 420 to 450 m, with a more depressed part at depths of ca. 550 m in an area 13.5 km west of the edge of the active Tregrosse Bank. The seafloor of the plateau adjacent to this part of the scarp is covered by up to 2 m high submarine dunes with wavelengths of around 200 m (Figs. 2C, E). Dune flanks facing south are dipping more gently than the north and northwestward-facing ones, indicating a current direction towards the north to northwest, which corresponds with the inflow of the NCJ (Fig. 1). Submarine dunes appear to be located at the current-facing flank of a south to north migrating sediment body. Stratal truncations at this upcurrent, submarine-dune covered flank (Fig. 2E) is interpreted to reflect active erosion. The submarine dune ridges bend slightly, indicative for a current diffraction when flowing from the open sea onto the plateau. Further evidence of the impact of bottom currents on this southern flank of the Queensland Plateau is a 400 to 500 m depression lining the scarp, which is interpreted as current moat (Fig. 2C).

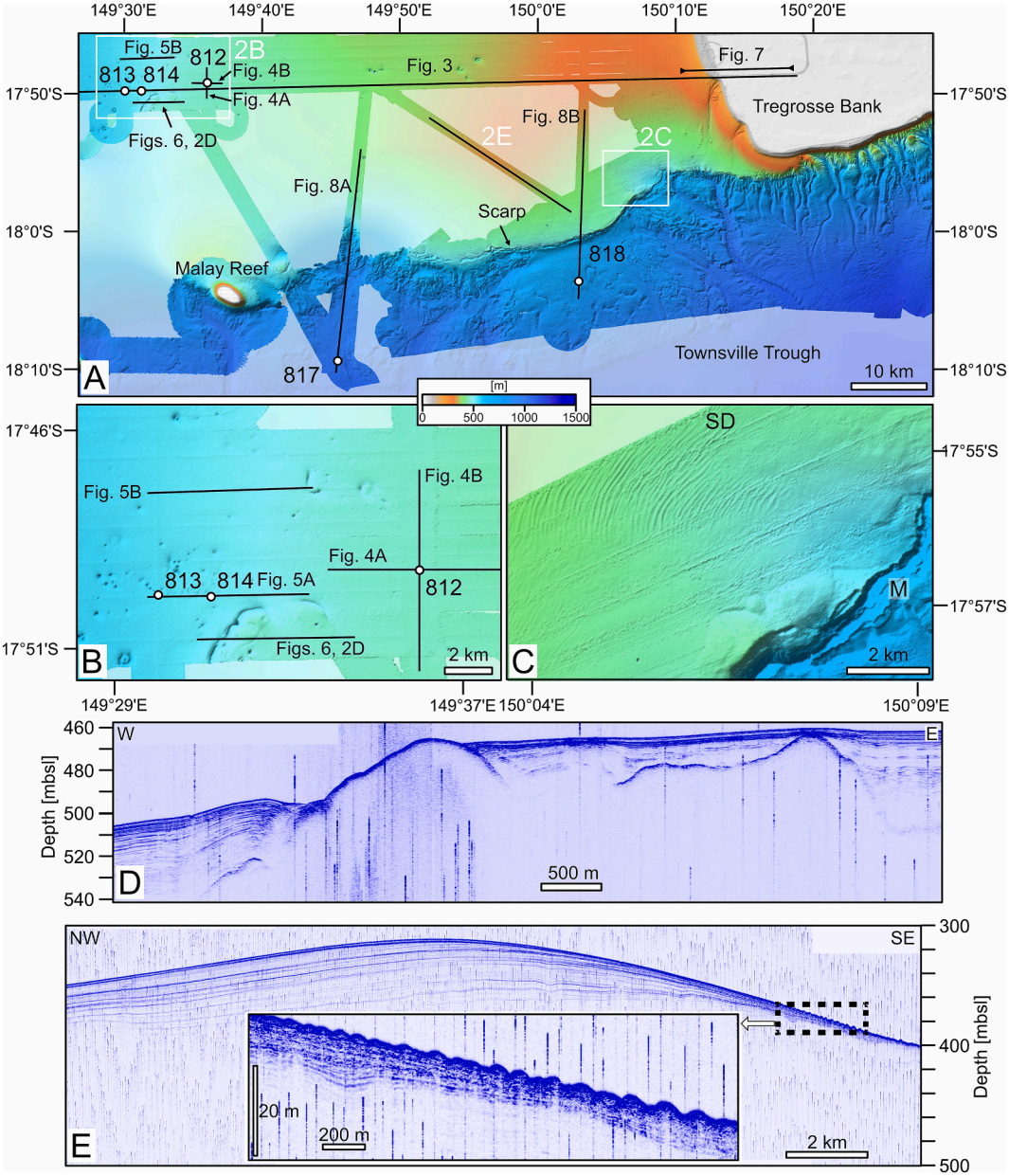

Fig. 2. A: Bathymetric data from the area west of Tregrosse Bank showing seismic lines from Cruise SO292 together with ODP sites. Multibeam data from RV *Sonne* Cruise SO292 merged with data from the RV *Falkor* cruises FK200429 and FK200802 (Siwabessy and Spinoccia, 2022). B: Seafloor morphology around sites 812 to 814 with seismic lines shown in the corresponding figures. Seafloor elevation with rounded shape in the south is interpreted to be a drowned atoll. Seafloor depressions are interpreted to represent fluid-flow extrusions, i.e. pockmarks. C: Detail of the scarp delimiting the platform west of Tregrosse Bank. Note the platform is covered by submarine dunes (SD). M: moat. D: Parasound profile through the seafloor elevation shown in B lined by a current moat. E: Parasound profile with submarine dunes and drift body. The stippled rectangle shows position of magnified area with submarine dunes and stratal truncations.

4.2. Depositional geometries

Line P05 is oriented west-east over a distance of ca. 100 km and covers inner parts of the Tregrosse Bank, its slope and the periplatform succession (Fig. 3). Ocean Drilling Program sites 813 and 814 are located in the western part of the line. The seismic signal is good within the upper 600–800 ms TWT, but degraded in the lower part of the succession. This is in areas that are interpreted to document rising fluids (chimneys). Some of these chimneys are connected with stacked v-shaped inflections of the seismic reflections, linked at the seafloor to the circular seafloor depressions (Figs. 2B, C). Locally, the basal contact of the post-rift sedimentary succession is imaged ("Basement Top", BT) at 1400–1600 ms TWT.

Basinwards, i.e. west of Tregrosse Bank major signal deterioration (blanking) is below a reflection with a strong contrast in acoustic impedance. The horizon mapped on this reflection is irregular, lying at a depth between 700 and 800 ms TWT. This surface correlates to what has been described as the top of the major carbonate bank covering larger parts of the Queensland Plateau (Davies et al., 1989, 1991) and is denominated herein as "Platform Top" horizon (PT). The edge of this platform, which is slightly elevated compared to the platform-interior strata, is located east of Site 814 (Fig. 3). Platform-internal geometries are described below, except one reflection termed herein as "Intra Platform" horizon (IP). These geometries and the IP horizon in part are poorly imaged in the seismic lines due to masking by the high-amplitude reflection but also by the seafloor multiple. Therefore horizons can only

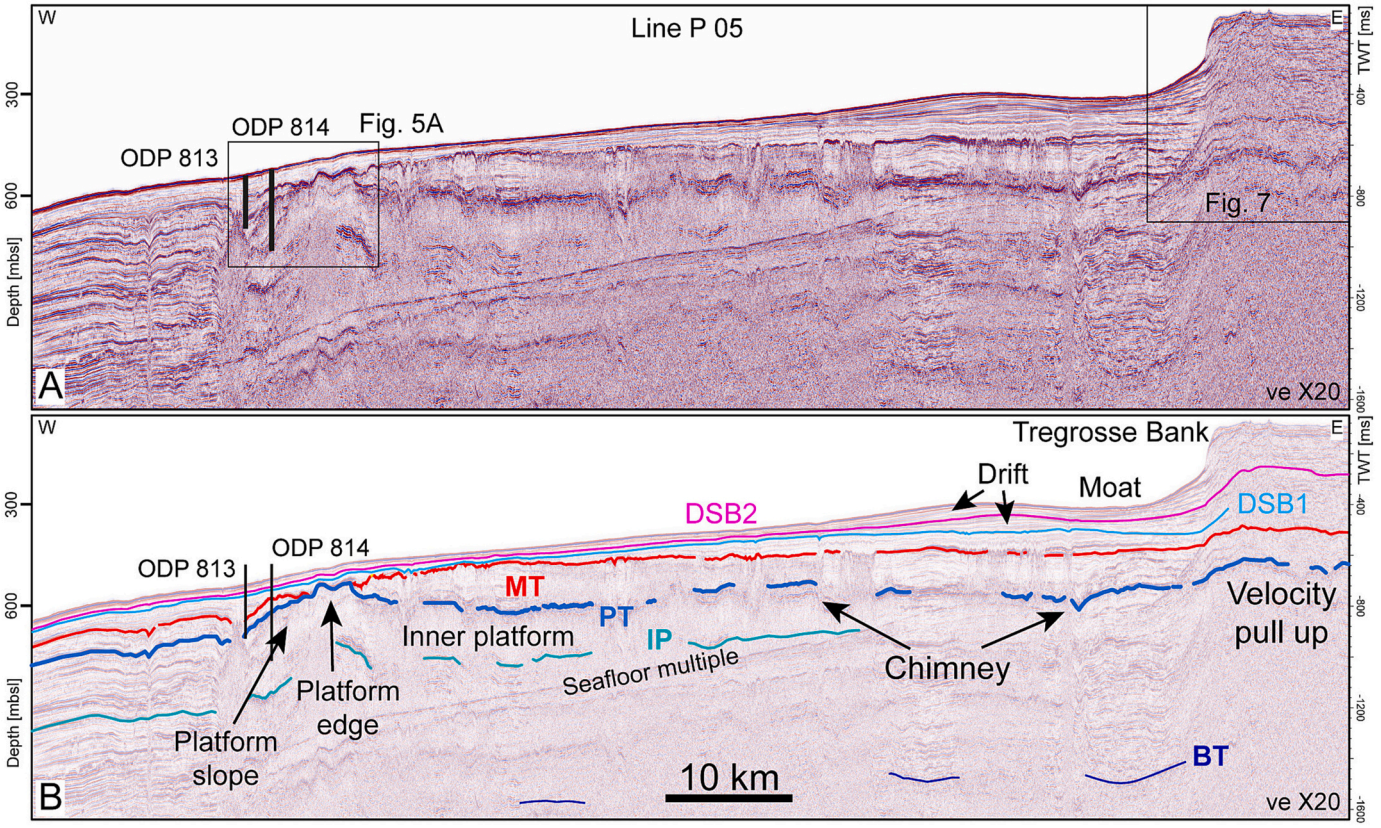

Fig. 3. A. Seismic line P05 running from the Queensland Trough into Tregrosse Bank with major unconformities (B). Note that the segment of the line below Tregrosse Bank is affected by a velocity pull up due to higher sound propagation velocities in the bank compared to the surrounding waters. See text for further explanations. Position of the line is shown in Fig. 2A.

be traced locally. West of the elevated platform edge, there are westward dipping layers. East of the platform edge in areas where blanking does not inhibit the recognition of reflections there is a subhorizontal layering, which corresponds to the platform-interior strata.

The seismic image is also deteriorated within the interior of Tregrosse Bank, mostly because of blanking below the high-amplitude reflection of the PT horizon, and also by the seafloor multiple (Fig. 3). Nevertheless, the PT horizon is still traceable below Tregrosse Bank and appears as an irregular horizon similar to the west of the bank. A ca. 150 ms TWT upward shift of this horizon in the time-migrated seismic section is interpreted to reflect a velocity pull-up due to increased interval velocity in the bank interior.

Overlying the irregular surface of the PT horizon, there is an interval with well-stratified medium-amplitude reflections, which thins out towards the elevated rim of the underlying drowned platform (Figs. 3, 4, 5A). It is bounded at the top by a horizon (Mound Top; MT) which is onlapped by the overlying deposits (Figs. 4, 5A). In seismic line P10, which runs north to south, this horizon is an undulating surface (Fig. 4B). The reflection packages are interpreted as submarine dunes or mounds. The unit delimited by PT and MT is denominated Mound Unit. The mounded bodies shown in Fig. 4B have a width of ca. 1.8 km and a height of ca. 100 m and internal reflections subdivide them into two units. A lower unit (LM) that consists of discontinuous subparallel strata, and an upper unit (UM) of convex-upward inclined beds arranged in a south progradational pattern. The mound unit merges with the PT horizon in the area east of the edge of the drowned platform.

West of this edge, i.e. in front of the drowned carbonate platform, the mound unit is wedge shaped, thickening to the west. In another section, which also cross-cuts the edge of the bank, the mound unit reflections onlap the PT horizon exhibiting a concave-upward shape (Fig. 5B).

Southeast of Site 813, in the area of the circular elevation (Fig. 2) the mound unit crops out at the seafloor (Fig. 6). The mound unit in line P09, which cross-cuts this feature appears to image a structure with two elevated margins, ca. 3300 m apart. The reflections in the structure are chaotic to discontinuous, with some better-defined layers between the margins. Taking into account the apparent circular shape of the high (Fig. 2B) this structure is interpreted to represent a drowned atoll.

The MT horizon between ODP sites 813 and 814 and Tregrosse Bank is generally flat, except for occasional depressions which in part are linked to the chimneys crosscutting the platform unit, but also the mound deposits and the overlying sedimentary succession (Fig. 3). The mound unit is 40 to 100 ms thick, being thinnest in the middle part of the seismic line shown in Fig. 3.

The thickness of the mound unit appears unchanged in the interior of Tregrosse Bank, where the velocity pull-up affects the imaged succession (Fig. 7). Internally, the mound unit below the Tregrosse Bank shows a low-relief carbonate bank (Fig. 7). The bank edge was located ca. 3 km east of the present-day bank edge, and the bank growth pattern was aggradational.

West of Tregrosse Bank the succession overlying the MT horizon is characterized by a series of medium amplitude continuous reflections, arranged in three concave-up 15 to 17 km wide bodies. Surfaces with lateral pinch outs and low-angle stratal truncations delimit these bodies. Bodies are around 60 ms TWT (ca. 55 m) thick and thin out towards the west to around 30 m at ODP Site 812 (Fig. 3) and to the east, before thickening under Tregrosse Bank (Fig. 3). There, the bedding changes to clinoforms interpreted as bank slope deposits. This stratal arrangement is interpreted to reflect a system of sheeted to mounded drifts separated from the carbonate bank by a moat. Through time, the moat has migrated west around 5 km. The surfaces separating the drift bodies are herein named Drift Sequence Boundaries (DSB) 1 and 2.

Aggradational to retrogradational bank growth persisted during

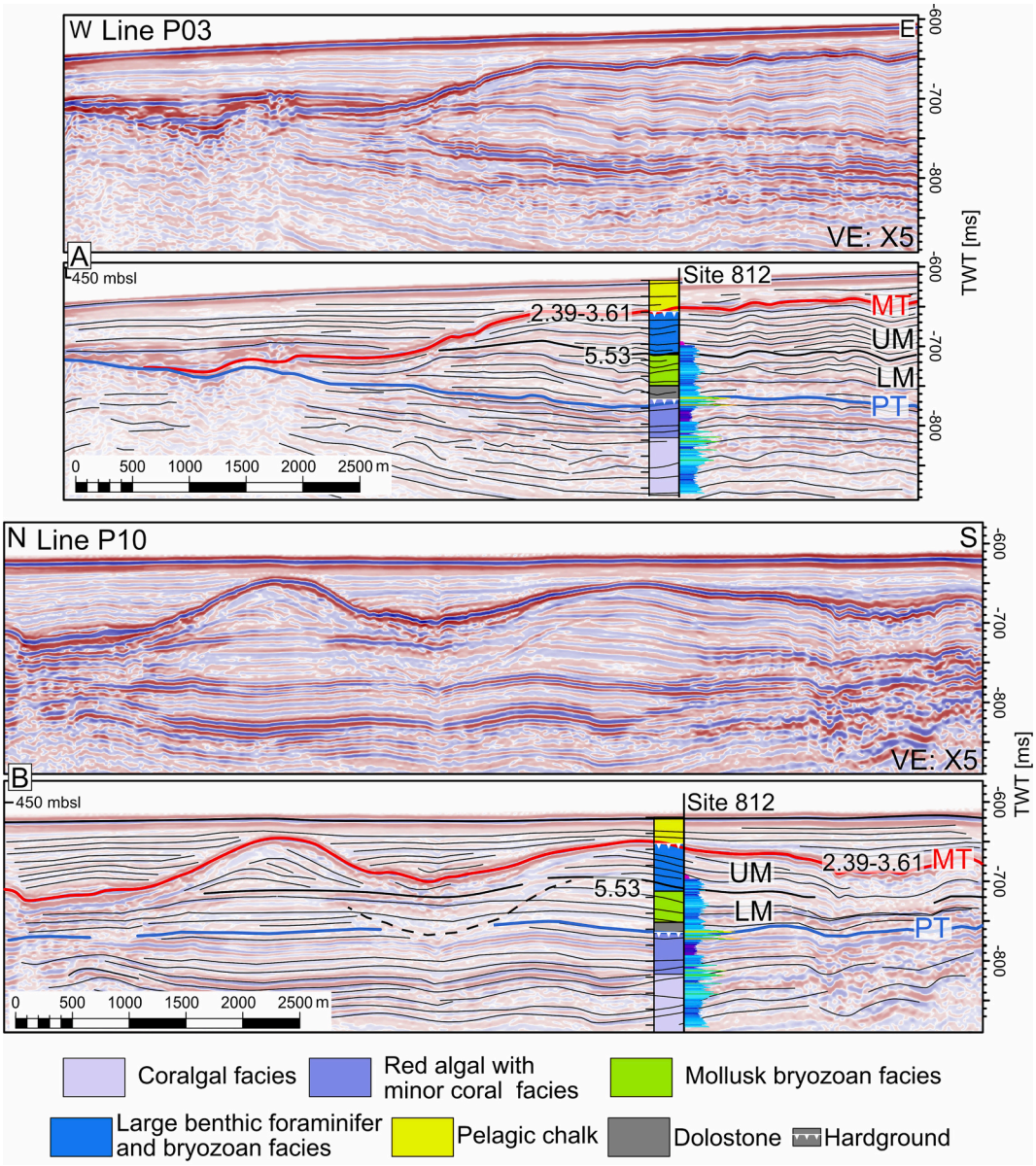

Fig. 4. A: Seismic line P03 running from the margin of the drowned bank east into the mound succession. Main facies at Site 812 and gamma-ray log are shown (for detail see Suppl. 2); ticks left of the column indicate 20 m intervals. B: Seismic line P10 with mound-shaped bodies showing internally dipping reflections. The stippled line indicates position of a peg-leg multiple. MT: Mound Top horizon, PT: Platform Top horizon, LM: lower mound unit, UM: upper mound unit. The position of lines in A and B shown in Fig. 2B. Numbers correspond to ages in millions of years, see Supplement 2 and text for more detail.

deposition of the lower drift package, which was followed by a back-stepping or a flattening of the depositional relief during formation of the second drift package (Fig. 7). Bank-edge progradation finally started during deposition of the third and uppermost drift package.

Fig. 8 displays two seismic lines through the southern edge of the plateau and towards the Townsville Trough. Line P13 covers a south to north transect with ODP Site 817, located in the Townsville Trough (Fig. 8A). The PT and the MT horizons can be traced to the plateau edge. Downslope, the strata dip towards the Townsville Trough and are therefore interpreted as platform slope deposits. Layering, however, is discontinuous and contorted, and there are offsets interpreted to trace planes of submarine landslides. The IP and PT horizons can be followed to some degree down to ODP Site 817. The MT horizon, however, is not possible to be traced because of the contorted stratification of the slope succession (Fig. 8A).

The reflection pattern north of the plateau edge appears chaotic to discontinuous for the platform deposits (Fig. 8A). This is interpreted to represent the shallow-water succession of the platform, possibly with reef deposits and a diagenetic overprint by karstification. The succession overlying the PT horizon is layered, thinning out towards the edge of the plateau.

Line P11 covers a south to north transect from ODP Site 818 in the Townsville Trough onto the Queensland Plateau (Fig. 8B). On the plateau, the PT and the MT horizons can be traced almost to the plateau's edge, where finally a blanking inhibits further identification. The mound unit is a wedge with an irregular outline thinning out away from the platform edge. Internally, the wedge contains low angle dipping continuous to discontinuous reflections downlapping onto the PT horizon. The nature of the deposits cannot be resolved with the available data. The lateral change in thickness together with the seismic facies change from discontinuous to rather layered reflections is taken as an indication that there was an in-situ carbonate production (e.g. a reef or similar) at the edge of the plateau.

The toe of slope deposits imaged in Line P11 are formed by a

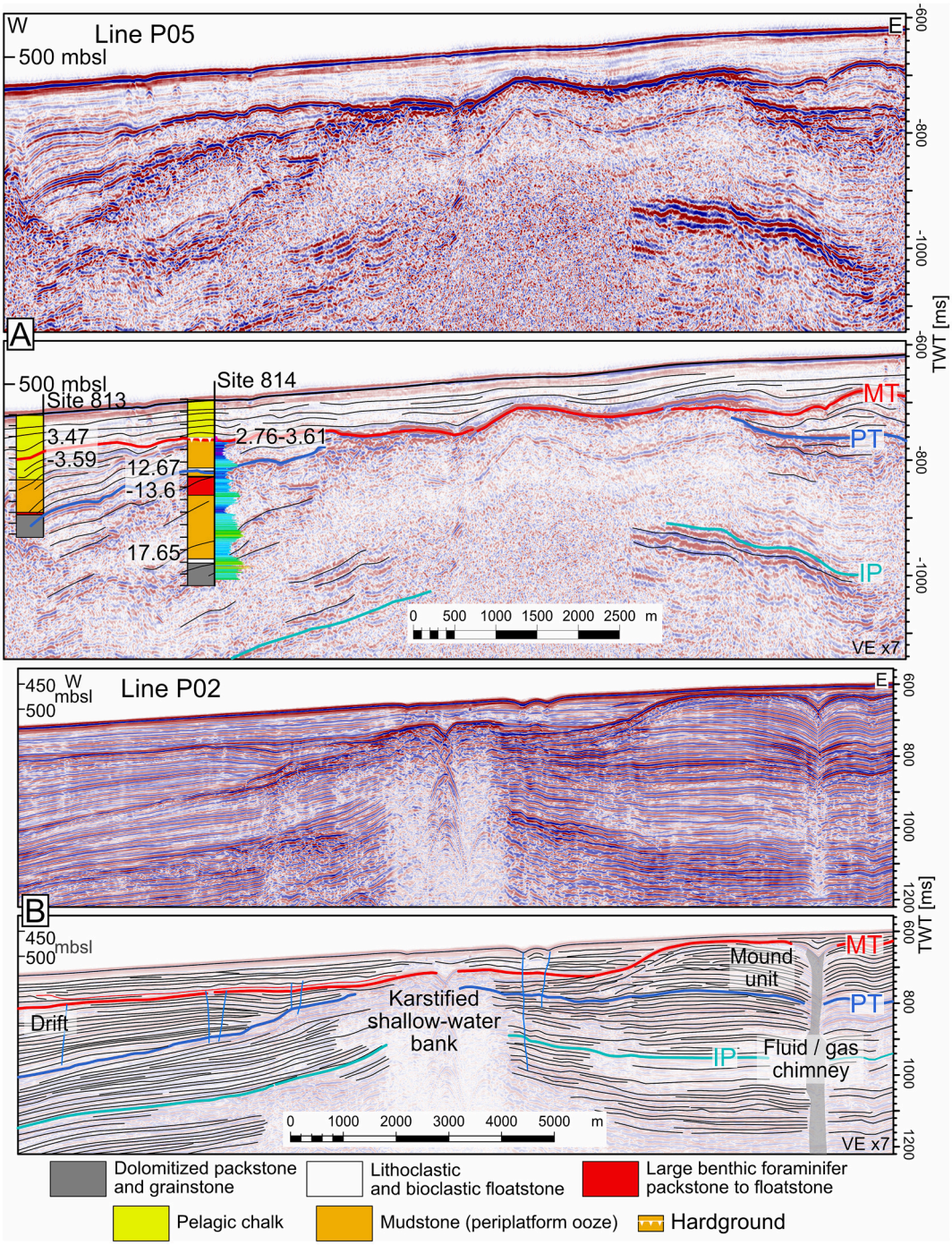

Fig. 5. A: Seismic line P05 crossing the positions of sites 813 and 814 and the margin of the drowned platform. Main facies are shown for both sites. Downhole gamma ray logging was performed at Site 814 (for detail see Suppl. 3). B: Seismic line P02 crossing the margin of the drowned bank north of line P05. Blue line: Platform Top horizon; red line: Mound Top horizon; Cyan line: Intra Platform horizon. Positions of lines are shown in Fig. 2B. . Numbers correspond to the ages in millions of years, see Supplement 3 and 4 as well as text for more detail. (For interpretation of the references to colour in this figure legend, the reader is referred to the web version of this article.)

succession of contorted and continuous reflections. The intervals consist of continuous reflections that in part form packages with concave-up geometries, such as for example in the youngest part of the succession. In Fig. 2B and D the seafloor displays a moat that lines the edge of the drowned bank. Therefore, the toe of slope succession is interpreted to consist of an alternation of drift deposits and mass transport complexes.

There are several indicators that the deposits overlying the drowned parts of the bank have been deposited under the influence of bottom currents. The deposits overlying the bank at ODP Site 812 exhibit mound-shaped, larger benthic foraminifer and bryozoan facies (Supp. 2) with internally inclined layering (Fig. 4B). The internal structure of the mounds is comparable to the structure of Danian bryozoan mounds in the Danish Basin (Anderskouv et al., 2007; Bjerager and Surlyk, 2007). There, the main current system is described to impinge on the steep flank of the mounds, where preferential conditions favor bryozoan growth, i.e. progradation of the mounds was against the prevailing bottom current.

Further, the wedge deposited in front of the bank edge has the

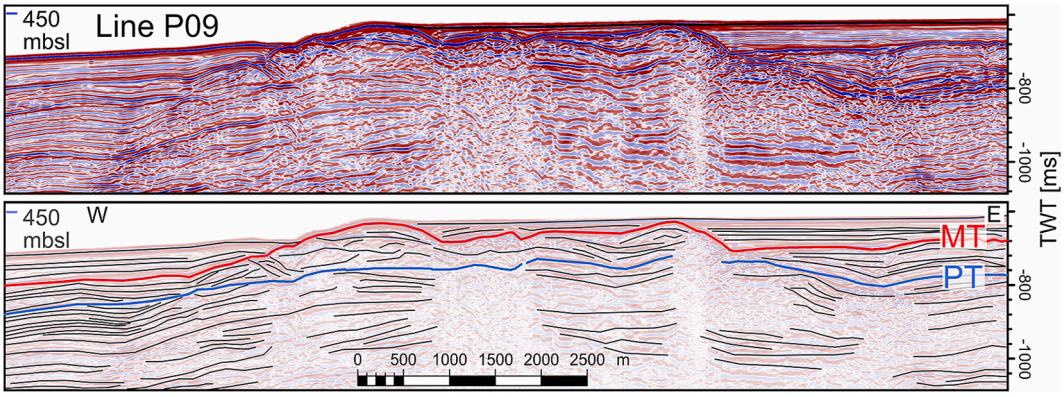

Fig. 6. Seismic line P09 with drowned atoll-like structure south of sites 813 and 814. The position of the line is shown in Fig. 2B.

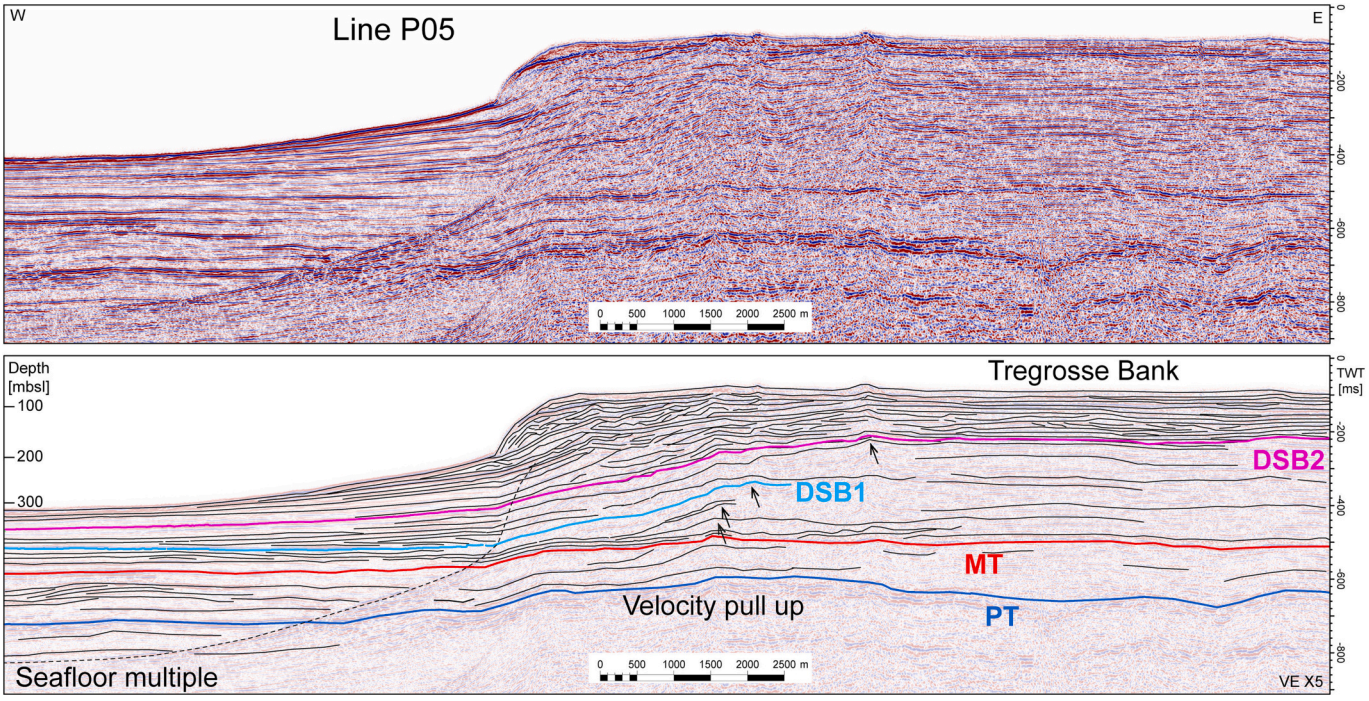

Fig. 7. Part of W-E seismic line P05 with detail of the stratigraphy of Tregrosse Bank. The mound unit does not show major lateral variations in thickness. Above the Platform Top horizon, the growth pattern of the bank is first aggradational, changing into a retrogradation at DSB1 before the bank edge started prograding above DSB2. The position of line P05 is shown in Fig. 2A. Dashed line: seafloor multiple.

geometry of a mounded drift (Fig. 5B). The layers in the lower part of the sediment wedge located basinward of the drowned platform edge onlap the PT horizon and are down-bended towards this surface. This is interpreted as a drift and moat geometry.

4.3. Seismic to well correlation

4.3.1. Sedimentary facies

4.3.1.1. ODP Site 812. The lower 158 m of the succession at ODP Site 812, which is located in a present-day water depth of 462 m, is an alternation of dolomitized wackestone to floatstone (Fig. 4, Suppl. 2). Major components are coral debris, green algae (*Halimeda*), red algae, bryozoa, large benthic foraminifers (*Amphistegina, Lepidocyclina*), in the upper 40 m red algae and mollusks dominate (Suppl. 2). The depositional environment has been interpreted as deep to shallow lagoonal and shallow water close to a reef (Davies et al., 1991). This part of the succession has been previously defined as lithostratigraphic Unit III with a phosphatic-goethitic hardground at the top (Suppl. 2). The position of the hardground correlates with an abrupt uphole reduction of the gamma ray values. Lithostratigraphic Unit III contains abundant moldic porosity which has been attributed to meteoric diagenesis (Davies et al., 1991). The hardground correlates to the PT horizon (Fig. 4).

The overlying Unit II is a sucrosic dolomite in the lower part of the unit, changing up-section into packstone to floatstone with bryozoan, mollusks, echinoderm debris, and benthic foraminifers. This interval is overlain by floatstone and wackestone with large benthic foraminifers (*Cycloclypeus*, *Operculina*, *Amphistegina*, and *Lepidocyclina*), bryozoa together with other benthic foraminifers and planktonic foraminifers (Davies et al., 1991; Betzler, 1997). The top of Unit II is a hardground with carbonate fluorapatite, ferroan to nonferroan dolomite, marine sparry calcites, and goethite with minor amounts of gibbsite interpreted to have resulted from current winnowing and erosion (Glenn and Kronen Jr., 1993). The succession terminating in the hardground has been interpreted as being formed by a warm-temperate carbonate factory in view of the presence of very minor corals and calcifying green algae

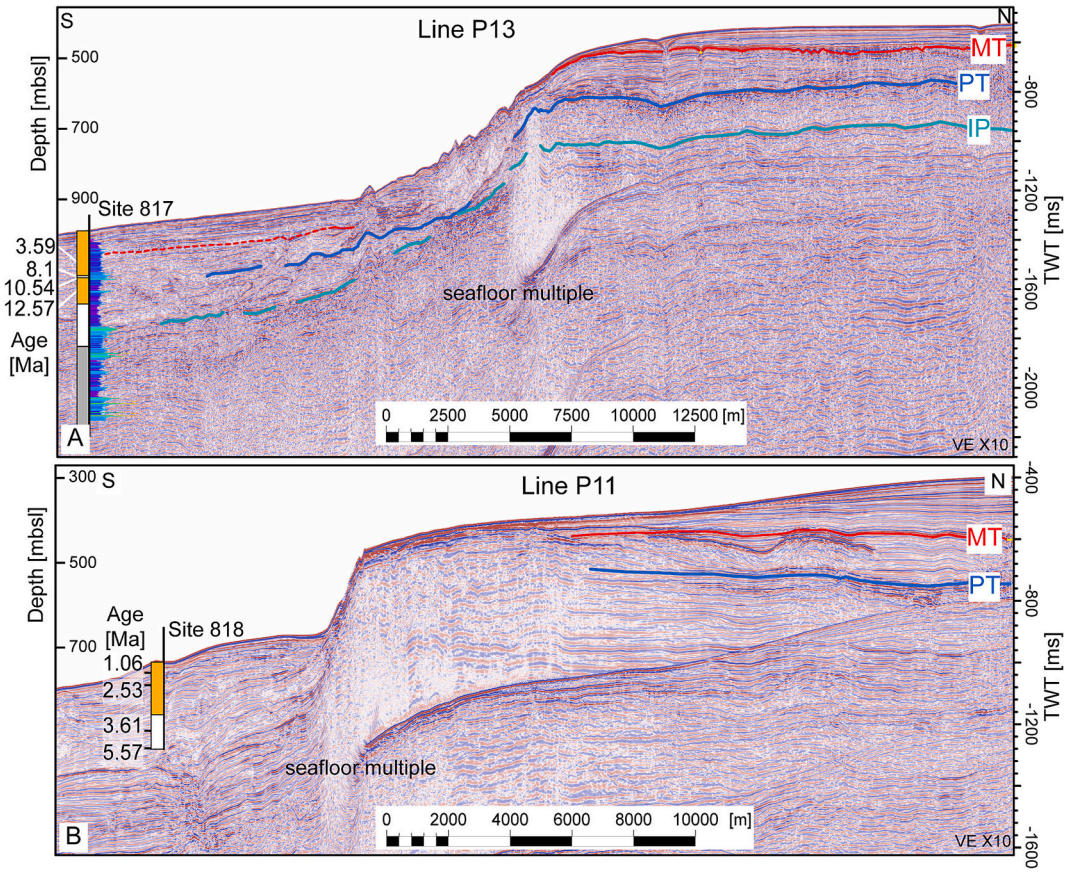

Fig. 8. Seismic lines P13 and P11 crossing the southern margin of the platform west of Tregrosse Bank with main facies at sites 817 and 818. Gamma-ray log for Site 817 is shown, see Suppl. 5 for details A: Correlation of horizons from the platform down into the Townsville Trough is interpretative, as a series of mass transport complexes in front of the margin of the drowned platform hampers a clear correlation of individual reflections. B: Correlation of reflections from the plateau into the Townsville Trough is not possible because of the blanking in the margin zone of the drowned platform. The position of lines is shown in Fig. 2A. Blue line: Platform Top horizon; red line: Mound Top horizon; cyan line: Intra Platform horizon. (For interpretation of the references to colour in this figure legend, the reader is referred to the web version of this article.)

(Betzler, 1997). The hardground correlates with the position of the MT horizon, the contact between the mollusk-rich facies, and the LBF – bryozoan facies coincides with the base of the mound-shaped deposits (Fig. 4).

4.3.1.2. ODP sites 813 and 814. At the more proximal ODP Site 814 (water depth: 520 m) the lower part of the succession consists of dolomitized packstone and grainstone, which is overlain by a 7 m thick lithoclastic and bioclastic floatstone to rudstone interval (Fig. 5, Suppl. 3). In seismic line P05, the contact between both lithologies correlates with the top of a seismic package with dipping discontinuous high amplitude reflections which is overlain by a package of lower amplitude chaotic reflections.

Overlying the floatstone and rudstone, there is a 100 m thick mudstone interval with planktonic foraminifers, which has been interpreted as periplatform ooze (Davies et al., 1991). This is followed by a 30 m thick large benthic foraminifer (*Lepidocyclina, Cycloclypeus, Operculina, and Amphistegina*) packstone to floatstone, which was interpreted as sediment gravity flow deposits (Davies et al., 1991). The lithological change in the seismic data is imaged by a change from the low amplitude to a higher amplitude chaotic seismic facies. The base of the large benthic foraminifer packstone to floatstone coincides with the PT horizon (Fig. 5A). The remaining part of the succession consists of a series of hemipelagic to pelagic carbonate ooze and chalk, interrupted by a floatstone layer rich in neritic components and a phosphatic hardground (Fig. 5A). The position of the hardground correlates with the MT horizon.

At ODP Site 813 (water depth: 539 m), the lower part of the sedimentary succession is a dolomitized grainstone (Fig. 5A, Suppl. 4). The top of this sediment package coincides with the PT horizon and is overlain by a thin interval of a rudstone with large benthic foraminifers. The remaining part of the succession is formed by hemipelagic and pelagic carbonate ooze and chalk.

4.3.1.3. ODP site 817 and 818. At ODP Site 817 a 657 m deep hole was drilled and cored, although core recovery in the lower part of the well was poor (Davies et al., 1991). The upper part of the succession, down to 200.8 mbsf is a nannoplankton and planktonic foraminifer ooze (Fig. 8A, Suppl. 5). Downhole, the ooze changes to chalk, and below ca. 300 mbsf the succession is an alternation of chalk and bioclastic packstone and grainstone. The lower part of the well finally consists of bioclastic packstone and grainstone and of dolomite in its lowermost part. The gamma-ray log down to 396 mbsf, which approximately corresponds to the depth of the projected IP horizon, fluctuates, before changing to generally lower values in the upper part of the succession (Suppl. 5). In this interval, there are gamma ray excursions around 269 mbsf and 225 mbsf. The top of this upper excursion coincides with a hiatus of 2.4 million years.

At ODP Site 818 the well penetrated 303 m of sediment (Davies et al., 1991). The upper 200 m of the succession is a calcareous nannofossil ooze and chalk, with interbedded calciturbidites and slumps in the lower part (Fig. 8B, Suppl. 6).

4.3.2. Ages of sedimentary breaks at sites 812 to 814

The age of the seismic horizon MT is well-defined at ODP Site 812. There, this horizon lies at a depth of 27 to 29 mbsf (Fig. 4; Suppl. 2). The succession at a depth of 28 mbsf contains a phosphatic hardground, which here is interpreted to correspond to this seismic horizon. The age of the deposits is between 2.39 Ma and 3.61 Ma. A maximum age of 3.61 Ma is therefore proposed for the demise of mounds recorded at ODP Site 812.

At ODP Site 814, a hardground is recorded from the position of the correlative seismic horizon of the MT horizon, and located at a depth of 57 mbsf (Supp. 3), which corresponds to a high-amplitude reflection in the seismic data. The age of these deposits is bracketed by assignments of 2.76 Ma and 3.61 Ma respectively (Suppl. 3). At ODP Site 813, the same horizon lying at a depth of ca. 67 mbsf is bracketed between a datum of 3.47 Ma and 3.59 Ma (Suppl. 4). Within the possible dating accuracy this is considered to be consistent and therefore an age of 3.47 Ma to 3.61 Ma is proposed for this sedimentological break.

The age of the seismic horizon separating the carbonate platform from the mound succession, the PT horizon, is not datable at ODP Site 812, as no biostratigraphic datums were identified in the corresponding succession. At a depth of 275 mbsf, i.e. ca. 70 m below the seismic horizon, the large benthic foraminifer *Nephrolepidina howchini* was found, which is indicative of a middle Miocene age (Gartner et al., 1993). At ODP Site 814 the PT horizon just underlies strata dated as 12.67 million years old (Suppl. 3). Ten meters below, an age of 13.6 Ma was determined. No age diagnostic microfossil could be determined at a depth of around 178 mbsf at ODP Site 813, i.e. the position of this seismic reflection (Suppl. 4). The top of the carbonate platform (PT horizon) thus is 12.67–13.6 Ma old, i.e. around 13 Ma.

The ages of the two unconformities which subdivide the drift succession can be assessed based on biostratigraphic data at ODP Site 814 (Suppl. 3). The DSB 1 unconformity lies just below of a datum of 1.93

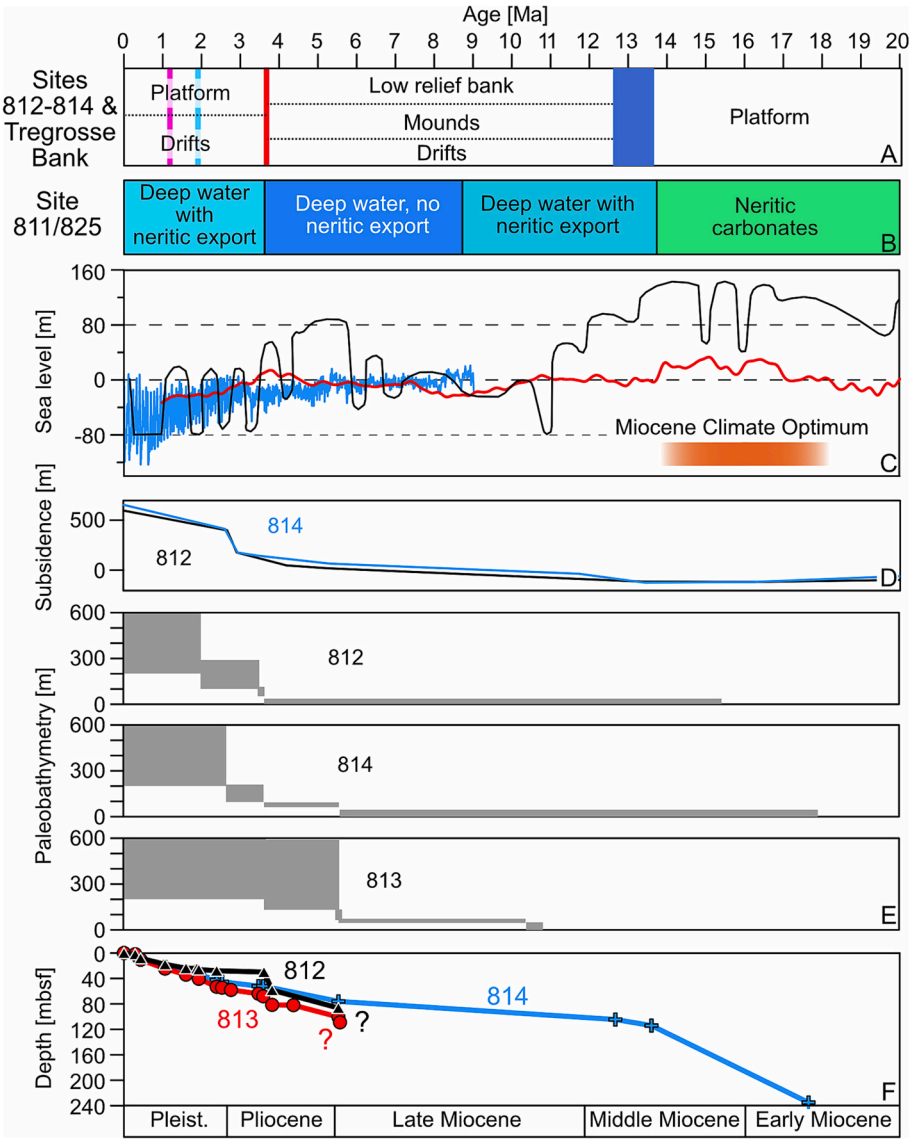

Fig. 9. A: Main breaks of changing carbonate platform configuration in the area of Tregrosse Bank near sites 812–814. Blue line: Platform Top horizon; red line: Mound Top horizon; light blue line: DSB1; purple line: DSB2. B: Sediment export variations from Holmes Reefs near site 811/825 (for location see Fig. 1A) reflecting the conditions at the upper part of the pinnacle-shaped body (after Droxler et al., 1993). C: Eustatic sea-level variations. Blue and red lines: Miller et al. (2020); black line: Haq et al. (1988). D: Tectonic subsidence at sites 812 and 814 including eustatic sea-level variations (Müller et al., 2000). E: Reconstruction of the paleobathymetry at sites 812, 813 and 814 based on benthic foraminifera (Katz and Miller, 1993). F: Age-depth plots for sites 812, 813, and 814 based on biostratigraphic data in Davies et al. (1991) and Gartner et al. (1993). (For interpretation of the references to colour in this figure legend, the reader is referred to the web version of this article.)

Ma. The upper DSB 2 unconformity lies just above a 1.6 Ma datum.

5. Discussion

5.1. General evolution of the Queensland Plateau carbonate banks

The correlation of ODP Leg 133 sites 812 to 814 lithostratigraphy together with the RV *Sonne* seismic stratigraphy provides a reorganization of the Queensland Plateau carbonate platform during the Neogene (Fig. 9). Extensive bank growth (see Fig. 1 for bank outlines) was interrupted during the early Late Miocene, after the Miocene Climate Optimum. Meteoric diagenesis in the interval just below the PT horizon, as recorded at ODP Site 812, indicates that the first step leading to this interruption possibly was a partial subaerial exposure (Davies et al., 1991), probably triggered by a global sea-level drop (Fig. 9). Biostratigraphic data do not allow to resolve when the platform was reflooded after this emersion. At ODP Site 814, between 76 mbsf and 104.5 mbsf (5.53–12.57 Ma), there is an interval with no datable fossils. Nannoplankton associations were described as consisting of generalized species that probably were associated with marginal or possibly relatively cool surface waters (Davies et al., 1991).

Fig. 9 summarizes the age-depth plots based on the biostratigraphic data presented in the Leg 133 site reports (Davies et al., 1991) and in Gartner et al. (1993). The relevant interval above the PT horizon appears to be characterized by a reduced sedimentation rate, although it cannot be excluded that there was also a phase of non-deposition.

Depositional geometries as imaged in RV *Sonne* seismic lines show that Late Miocene platform shrinking was not a consequence of a simple margin backstepping (Figs. 3–5). The demise of the middle Miocene platform between 13.6 Ma and 12.67 Ma was followed by a depositional episode with a co-existence of small relict banks, i.e. the drowned atoll shown in Figs. 2C and 6, current-controlled mounds (Fig. 4A) and a low relief bank (Figs. 3, 7), now buried below Tregrosse Bank. Bank growth of the Tregrosse Bank was initiated with an aggradational mode, before a bank-edge progradation started ca. 1.1 million years ago.

Partial drowning affected several of the carbonate banks on the Queensland Plateau (Fig. 1; Mutter, 1977, Davies et al., 1989). The reduction in shallow-water platform area appears to have been most pronounced on the western sides, in the case of the Tregrosse-Coringa and Diane banks (Fig. 1B), as also depicted in Davies et al. (1989).

5.2. Controlling factors of platform evolution

In an earlier study the deposits overlying the PT horizon at ODP sites 813 and 814 were interpreted as a carbonate ramp (Betzler, 1997). The data introduced herein draw a different picture and identify deposits overlying the drowned bank as a current-controlled depositional package. Sediments in front of the abandoned platform are arranged in drifts and their associated moats. Paleowater depth during deposition of these sediments was inner neritic at ODP Site 814 and middle neritic at ODP Site 813 (Katz and Miller, 1993, Betzler, 1997; Fig. 9). Overlying the top of the drowned platform, deposits were accumulated in mounds, with southward dipping internal bedding. At ODP Site 812, these sediments contain up to 50% of bryozoans, together with larger benthic foraminifers as well as other benthic and planktonic foraminifers (Betzler, 1997). The enrichment in bryozoans is taken here as an indication that the carbonate factory of the mound facies was heterotrophic to mixotrophic, with only very minor amounts of corals (Suppl. 2). Water depth was inner to middle neritic (Katz and Miller, 1993).

Changes in water temperature were called upon to trigger the partial drowning of the Queensland Plateau carbonate banks. However, two opposite interpretations were presented: a cooling was proposed by Betzler et al. (1995) and Isern et al. (1996), a warming by Petrick et al. (2023). Today, yearly mean surface-water temperatures are between 26° and 27 °C, and around 25 °C at a water depth of 49 m (ereefs.aims.gov.au). Water temperature at a depth of 200 m is around 21 °C (Betzler et al., 2022).

The cooling after the Miocene Climate Optimum was reconstructed based on oxygen isotope data (Isern et al., 1996), on the occurrence of frequent *Bolboforma* microfossils in Site 813 deposits (Betzler et al., 1995) in the interval delimited by the PT and MT horizons, and on the neritic facies at Site 812 with only minor corals or calcareous algae indicative of warm waters (Betzler, 1997; Supp. 2). *Bolboforma* is a problematic microfossil, which outside the Southern Ocean has been proposed to define the pathway of Southern Component Intermediate Water (Cooke et al., 2002; Crundwell et al., 2005). The marginal or cool-water calcareous nannoplankton assemblages reported for this time interval from Site 813 (Davies et al., 1991) would be an additional and independent indication of lowered water temperatures.

At ODP Site 811 water temperatures between 27° and 32 °C were reconstructed for the time between ca. 10.7 Ma and 7.3 Ma using the TEX_{86}^{H} molecular paleothermometer (Petrick et al., 2023), although the stratigraphic resolution of this study does not allow to gather data on the Degree Heating Week, i.e. the accumulation of HotSpots of 1 °C or greater through a rolling 12-week period, which appears to control coral bleaching and thus resilience of coral reefs to elevated temperatures (Heron et al., 2016).

An important point in the discussion about potential water temperature effects on the evolution of the Queensland Plateau shallow-water carbonate factories is the swift northward movement of the Australian Plate since the Miocene. Applying the latitude/longitude corrections as presented in van Hinsbergen et al. (2015), the ODP site transect analyzed herein was located around 23° S 15 million years ago, i.e. ca. 6° farther south than today, at the southern reach of Late Miocene trade winds (Groeneveld et al., 2017) and potentially located in cooler waters.

Droxler et al. (1993) introduced eustatic sea-level changes as a controlling mechanism for the late Pliocene re-initiation of a major shallow-water carbonate platform by using the increased influx of bank-derived carbonate in the deeper-water sites 811 and 817. At Site 811 located at the windward flank of Holmes Reef (Fig. 1A for location) and recording the off-bank shedding of shallow-water components, there was no or a very reduced platform export between 8.8 Ma and 3.5 Ma (Fig. 9). At the leeward side of Holmes Reef (Site 824), a similar interval with no influx of shallow-water export was recorded between ca. 8 Ma and 5.5 Ma (Davies et al., 1991), but dating of these deposits is poor.

The demise of the Middle Miocene platform correlates with the termination of a sea-level fall (Fig. 9). Haq et al. (1988) proposed further lowerings of eustatic sea level, with a maximum lowstand at 11 Ma, whereas Miller et al. (2020) show a trend of minor sea-level fluctuations between 13.5 and ca. 10 Ma, before a drop with a maximum at 8.3 Ma occurred. None of both sea-level trends appears to be reflected by the changes in depositional geometry and the changes in facies on the southern Queensland Plateau (Fig. 9).

Accommodation is not only controlled by the global sea level, but also by tectonic movements. Müller et al. (2000) calculated the subsidence rates for several of the ODP sites on the Queensland Plateau. At sites 812 and 814 the subsidence rates were determined as low, accelerating around 3 Ma (Fig. 9). Therefore, the subsidence is not seen here as a major driver of the platform to mound facies transition and the shrinkage of the Miocene platform. Differential subsidence of different areas of the Queensland Plateau, i.e. in fault-controlled blocks, is not documented for the Queensland Plateau (Mutter, 1977; Davies et al., 1989) and in our data. Based on modeling, DiCaprio et al. (2010) see the long-term dynamic subsidence with a tilting of Australia towards the northeast as related to the overriding of a subducting slab as a major driver for the platform drowning. Our data do not allow to verify this hypothesis.

Elevated nutrient influx has been evoked as a potential driver for carbonate platform drowning (Hallock and Schlager, 1986). Currently, there are no data available to reconstruct Miocene nutrient contents in the Queensland Plateau area. Chlorophyll-a concentrations for the year, 2019 are around 0.2 to 0.4 mg Chl $m^{-}3$ (ereefs.aims.gov.au).

In summary, none of the discussed potential controlling factors appears to turn out as sole or major driver of the presented carbonate platform evolution.

5.3. Current control on platform development?

The interaction of ocean currents with carbonate platform facies distribution and also the evolution of platforms has been discussed in a number of studies, based on data from the Bahamas (Mullins et al., 1980; Anselmetti et al., 2000; Betzler et al., 2014; Chabaud et al., 2016; Wunsch et al., 2018), from the Maldives and the Mascarenes (Betzler et al., 2009, 2021), from NW Australia (Bachtel et al., 2010; Rankey, 2020; Thronberens et al., 2022), and from NE Australia (Isern et al., 2004; John and Mutti, 2005; Eberli et al., 2010). It was shown that slopes are shaped by currents and that the onset of ocean currents trigger carbonate platform drowning (Betzler et al., 2009, 2023; Ling et al., 2021; Reolid et al., 2020; Isern et al., 2004; John and Mutti, 2005; Eberli et al., 2010). These processes induced a global Miocene turnover of the carbonate platform characteristics (Betzler and Eberli, 2019).

Located just 300 km south of the ODP sites 812 to 814 on the Queensland Plateau, the Marion Plateau was one of the key areas where this context has been elaborated (Isern et al., 2004, John and Mutti, 2005, Eberli et al., 2010). The platform demise of the northern part of the Marion Plateau is registered at a sequence boundary dated as having been formed at 13.5 Ma (Bashah et al., 2024). The southern part of the plateau drowned during the late Miocene (ca. 7 Ma). Based on core data from ODP Leg 194 and starting at 13.6 Ma the top and the flanks of the plateau were swept by currents stronger than before the formation of this boundary (John and Mutti, 2005). As a consequence of strengthened currents, sediment drifts formed in front of the drowned banks of the Marion Plateau (Isern et al., 2004; Eberli et al., 2010; Bashah et al., 2024).

Given the proximity of the Queensland and Marion plateaus which are both under the influence of the same current system (Fig. 1B), the age coincidence of the sedimentary breaks, i.e. the partial drowning events, is interpreted to reflect a common trigger. This is supported by the observation that current-controlled sedimentary patterns start to appear in the sedimentary record above the Platform Top horizon around 13 Ma (Figs. 3–5).

The remaining question is, whether currents alone can act as a trigger of carbonate platform decay and drowning. As noted by Hata et al. (2017) not only the magnitude but also the direction and source of currents determine coral larval settlement because they likely influence the supply or removal of larvae, which, however, also appears to differ with coral species (Elmer et al., 2016). Some larvae are redistributed within the same reef, whereas others travel over certain distances. Larval settlement rates also appear to decrease with increasing current speed depending on the coral species (Harii and Kayanne, 2002). The physical action of currents may also be a factor, as sediment suspension and bedload may inhibit or reduce coral growth.

Ecological conditions suppressing the development of tropical reefs and carbonate factories may be an additional factor linked to ocean current flows. At ODP Site 812 the demise of the platform coincides with the change from a carbonate factory indicative of warm water conditions (chlorozoan factory sensu James, 1997; T-factory sensu Schlager, 2003) to a warm-temperate factory, i.e. a factory in the lower range of tropical conditions (Betzler, 1997; Schlager, 2005). A similar carbonate factory turnover has been observed in the case of the age-equivalent break at the Marion Plateau (Isern et al., 2004). Applying a spatial analysis approach, it has been shown that the sea-surface temperature seasonality is the dominating parameter discriminating the different shallow-water carbonate factories (Laugié et al., 2019).

Finally it has to be stated that the partial demise of the Queensland Plateau carbonate platform occurred during the global cooling which followed the Miocene Climate Optimum. This cooling and the intensification of global latitudinal temperature gradients resulted in an intensified trade wind belt (Groeneveld et al., 2017), which also controls the circum-equatorial currents. So, all the data presented in our study are in line with the scenario of a globally-controlled onset of stronger currents potentially bringing in cooler waters to the Coral Sea platforms of the Queensland Plateau, at least in its southern areas.

We also draw attention to the fact that circulation on the Queensland Plateau during the Miocene was also controlled by a change of the Coral Sea Basin paleogeography. With the northward movement of the Australian plate, the first emergences of the pre-collision complex of New Guinea have been dated as occurring ca. 12 million years ago (van Ufford and Cloos, 2005). Diversification rates of rodents are further in line with a rapid geological uplift during the late Miocene, forming the New Guinea highlands (Roycroft et al., 2022). The establishment of a distinct Coral Sea warm pool (Isern et al., 1996) may be linked to the establishment of this physical current barrier.

6. Conclusions

The shrinking of the shallow-water area of the Queensland Plateau banks between 13.6 and 12.7 Ma co-occurred with the termination of the Miocene Climate Optimum. Partial platform drowning coincided by the inception of depositional signatures reflecting the intensification of bottom-current activity. Overlying a drowning unconformity, current-controlled mounds with a fauna devoid of corals or calcifying green algae developed and drift deposits accumulated lining the drowned bank margins. From 12.7 to ca. 3.7 Ma the relict bank, which forms the core of the still active Tregrosse Bank was a low relief platform. The bank later first aggraded, then after an episode of margin retrogradation, bank margin progradation started around 1 million years ago. Local reduction of shallow-water carbonate platform areas, coincident with a similar evolution of a differential drowning in the area of the Marion Plateau just south of the Queensland Plateau is taken as an indication that a process acted, which at places inhibited reef growth. Fundamental changes in the water mass properties or a rise in sea level are not seen as a controlling factor of this evolution. We show that partial carbonate drowning occurred on the Queensland Plateau at the time of the onset of a strengthened ocean circulation. The Queensland Plateau is a further example of the important influence of currents on carbonate platform growth evolution since the late middle Miocene.

Supplementary data to this article can be found online at https://doi.org/10.1016/j.margeo.2024.107255.

Dedication

We dedicate this study to our dear colleague Dick Kroon. We got the sad news that Dick passed away while we were acquiring the seismic and hydroacoustic data for this study on the Queensland Plateau with RV *Sonne* in 2022. CB, together with Dick sailed as young scientists to the same area on ODP Leg 133 in 1989. This laid the fundamentals of this follow-up study. Later, we sailed together on two other IODP expeditions, analyzing the evolution of tropical carbonate platforms in the Caribbean and in the Indian Ocean. The many enthusiastic and insightful discussions with Dick were the foundation of the desire to better understand the interaction between palaeoceanographic changes and carbonate platform evolution. Working with Dick was always an incredibly positive experience always accompanied by his most acute sense of humor. We not only miss a colleague, but also a very good friend.

CRediT authorship contribution statement

Christian Betzler: Conceptualization, Formal analysis, Funding acquisition, Investigation, Methodology, Project administration, Supervision, Visualization, Writing – original draft, Writing – review & editing. **Christian Hübscher:** Formal analysis, Methodology, Visualization, Writing – original draft, Writing – review & editing. **Sebastian**

Lindhorst: Conceptualization, Data curation, Formal analysis, Funding acquisition, Methodology, Writing – original draft, Writing – review & editing. **Thomas Lüdmann:** Conceptualization, Data curation, Formal analysis, Funding acquisition, Methodology, Writing – original draft, Writing – review & editing. **Carola Hincke:** Formal analysis, Investigation, Writing – original draft, Writing – review & editing. **Robin J. Beaman:** Data curation, Methodology, Writing – original draft, Writing – review & editing. **Jody M. Webster:** Investigation, Writing – original draft, Writing – review & editing.

Declaration of competing interest

The authors declare the following financial interests/personal relationships which may be considered as potential competing interests:

Christian Betzler reports financial support was provided by Bundesministerium für Bildung und Forschung. If there are other authors, they declare that they have no known competing financial interests or personal relationships that could have appeared to influence the work reported in this paper.

Data availability

SEGY data have been uploaded in PANGAEA (14.11.2023) and are available under https://doi.pangaea.de/10.1594/PANGAEA.965100.

The link to the SO292 multibeam data is available under https://www2.bsh.de/daten/DOD/Bathymetrie/Suedpazifik/so292.htm.

Acknowledgements

We thank the officers and crew of RV *Sonne* for the unlimited support during Cruise SO292. The shipboard scientific party and the technicians with their assistance provided the solid fundament that helped to acquire the data used in this study; a big thank to all of them. The Schmidt Ocean Institute is thanked for the RV *Falkor* multibeam data acquired during cruises FK200429 and FK200802. We thank Parks Australia for the research permit for Cruise SO292 (permit EPBC 2022/9168). This study was funded through grant 03G0292A – ICECARB from the Federal Ministry of Education and Research. Many discussions with Gregor Eberli during the past years helped develop some of the ideas presented in this study. The reviews by Jean Borgomano, Stefan Back and François Fournier are gratefully acknowledged.

References

Anderskouv, K., Damholt, T., Surlyk, F., 2007. Late Maastrichtian chalk mounds, Stevns Klint, Denmark — combined physical and biogenic structures. Sediment. Geol. 200, 57–72.

Andrews, J.C., Clegg, S., 1989. Coral Sea circulation and transport deduced from modal information models. Deep-Sea Res. 36, 957–974.

Anselmetti, F.S., Eberli, G.P., Ding, Z.-D., 2000. From the Great Bahama Bank into the Straits of Florida: a margin architecture controlled by sea-level fluctuations and ocean currents Bull. Geol. Soc. America 112, 829–844.

Bachtel, S.L., Posamentier, H.W., Gerber, T.P., 2010. Seismic geomorphology and stratigraphic evolution of a Tertiary-aged isolated carbonate platform system, Browse Basin, North West Shelf of Australia—Part II. In: Wood, L.J., Simo, J.A., Rosen, N.C. (Eds.), Seis-Mic Imaging of Depositional and Geomorphic Systems, vol. 30. SEPM (Society for Sedimen-tary Geology), Gulf Coast Section, Tulsa, Oklahoma, USA, pp. 115–135.

Bashah, S., Eberli, G.P., Anselmetti, F.S., 2024. Archive for the East Australian current: carbonate contourite depositional system on the Marion Plateau, Northeast Australia. Mar. Geol. 107224 https://doi.org/10.1016/j.margeo.2024.107224.

Beaman, R.J., 2010. Project 3D-GBR: A high-resolution depth model for the Great Barrier Reef and Coral Sea. Marine and Tropical Sciences Research Facility (MTSRF). Project 2.5i.1a Final Report,. MTSRF, Cairns, Australia, p. 13. plus Appendix 1. 10.26186/5e2f8bb629d07.

Betzler, C., 1997. Ecological controls on geometries of carbonate platforms: Miocene/Pliocene shallow-water microfaunas and carbonate biofacies from the Queensland Plateau (NE Australia). Facies 37, 147–166.

Betzler, C., Artschwager, M., Becking, J., Bialik, O.M., Eggers, D., Eisermann, J.O., Falkenberg, P., Häcker, T., Hübscher, C., Hincke, C., Lahajnar, N., Lindhorst, S., Lüdmann, T., Maak, J.M., Maul, J., Petrovic, A., Reolid, J., Saitz, Y., Schmidt, M.C., Schönbeck, F., Schwarz, T., Strehse, V., Wasilewski, T., Welsch, A., 2022. Towards an understanding of carbonate platforms in the icehouse world, Cruise No. SO292, 15.05.2022 - 21.06.2022, Nouméa (New Caledonia) - Nouméa (New Caledonia), SONNE-Berichte. Begutachtungspanel Forschungsschiffe, Bonn, pp. 1–58. https://doi.org/10.48433/cr_so292.

Betzler, C., Brachert, T.C., Kroon, D., 1995. Role of climate in partial drowning of the Queensland Plateau carbonate platform (northeastern Australia). Mar. Geol. 123, 11–32.

Betzler, C., Chaproniere, G.C.H., 1993. Paleogene and Neogene larger foraminifers from the Queensland Plateau: Biostratigraphy and environmental significance. Proc. Ocean Drill. Proj. Sci. Res. 133, 51–66.

Betzler, C., Eberli, G.P., 2019. Miocene start of modern carbonate platforms. Geology 47, 771–775.

Betzler, C., Hübscher, C., Lindhorst, S., Lüdmann, T., Reijmer, J.J.G., Braga, J.-C., 2016. Lowstand wedges in carbonate platform slopes (Quaternary, Maldives, Indian Ocean). Depositional Rec. 2, 196–207.

Betzler, C., Hübscher, C., Lindhorst, S., Reijmer, J.J.G., Römer, M., Droxler, A.W., Fürstenau, J., Lüdmann, T., 2009. Monsoonal-induced partial carbonate platform drowning (Maldives, Indian Ocean). Geology 37, 867–870.

Betzler, C., Kroon, D., Gartner, S., Wei, W., 1993. Eocene to Miocene chronostratigraphy of the Queensland Plateau: Control of climate and sea level on platform evolution. Proc. Ocean Drill. Proj. Sci. Res. 133, 281–289.

Betzler, C., Kroon, D., Reijmer, J.J.G., 2000. Synchroneity of major late Neogene Sea level fluctuations and paleoceanographically controlled changes as recorded by two carbonate platforms. Paleoceanography 15, 722–730.

Betzler, C., Lindhorst, S., Eberli, G.P., Lüdmann, T., Möbius, J., Ludwig, J., Schutter, I., Wunsch, M., Reijmer, J.J.G., Hübscher, C., 2014. Periplatform drift: the combined result of contour current and off-bank transport along carbonate platforms. Geology 42, 871–874.

Betzler, C., Lindhorst, S., Lüdmann, T., Reijmer, J.J., Braga, J.-C., Bialik, O.M., Reolid, J., Eisermann, J.O., Emeis, K., Rixen, T., Bissessur, D., 2021. Current and sea level control the demise of shallow carbonate production on a tropical bank (Saya de Malha Bank, Indian Ocean). Geology 49, 1431–1435.

Betzler, C., Lindhorst, S., Reijmer, J.J.G., Braga, J.C., Lüdmann, T., Bialik, O.M., Reolid, J., Geßner, A.-L., Hainbucher, D., Bissessur, D., 2023. Carbonate platform drowning caught in the act: the sedimentology of Saya de Malha Bank (Indian Ocean). Sedimentology 70, 78–99.

Bjerager, M., Surlyk, F., 2007. Danian Cool-Water Bryozoan Mounds at Stevns Klint, Denmark–A New Class of Non-Cemented Skeletal Mounds. J. Sediment. Res. 77, 634–660.

Bostock, H.C., Opdyke, B.N., Gagan, M.K., Kiss, A.E., Fifield, L.K., 2006. Glacial/interglacial changes in the East Australian current. Clim. Dyn. 26, 645–659.

Brachert, T.C., Betzler, C., Davies, P.J., Feary, D.A., 1993. Climatic change: Control of carbonate platform development (Eocene-Miocene, Leg 133, Northeastern Australia). Proc. Ocean Drill. Proj. Sci. Res. 133, 291–300.

Brinkman, R., Wolanski, E., Deleersnijder, E., McAllister, F., Skirving, W., 2002. Oceanic inflow from the Coral Sea into the Great Barrier Reef. Estuar. Coast. Shelf Sci. 54, 655–668.

Ceccarelli, D.M., McKinnon, A.D., Andréfouët, S., Allain, V., Young, J., Gledhill, D.C., Flynn, A., Bax, N.J., Beaman, R., Borsa, P., Brinkman, R., Bustamante, R.H., Campbell, R., Cappo, M., Cravatte, S., D'Agata, S., Dichmont, C.M., Dunstan, P.K., Dupouy, C., Edgar, G., Farman, R., Furnas, M., Garrigue, C., Hutton, T., Kulbicki, M., Letourneur, Y., Lindsay, D., Menkes, C., Mouillot, D., Parravicini, V., Payri, C., Pelletier, B., Richer de Forges, B., Ridgway, K., Rodier, M., Samadi, S., Schoeman, D., Skewes, T., Swearer, S., Vigliola, L., Wantiez, L., Williams, A., Williams, A., Richardson, A.J., 2013. The Coral Sea. Adv. Mar. Biol. 66, 213–290.

Chabaud, L., Ducassou, E., Tournadour, E., Mulder, T., Reijmer, J.J.G., Conesa, G., Giraudeau, J., Hanquiez, V., Borgomano, J., Ross, L., 2016. Sedimentary processes determining the modern carbonate periplatform drift of Little Bahama Bank. Mar. Geol. 378, 213–229.

Choukroun, S., Ridd, P.V., Brinkman, R., McKinna, L.I.W., 2010. On the surface circulation in the western Coral Sea and residence times in the Great Barrier Reef. J. Geophys. Res. Oceans 115. https://doi.org/10.1029/2009JC005761.

Church, J.A., 1987. East Australian current adjacent to the Great Barrier Reef. Mar. Freshw. Res. 38, 671–683.

Colberg, F., Brassington, G.B., Sandery, P., Sakov, P., Aijaz, S., 2020. High and medium resolution ocean models for the Great Barrier Reef. Ocean Model 145, 101507.

Cooke, P.J., Nelson, C.S., Crundwell, M.P., Spiegler, D., 2002. Bolboforma as monitors of Cenozoic palaeoceanographic changes in the Southern Ocean. Palaeogeogr. Palaeoclimatol. Palaeoecol. 188, 73–100.

Crundwell, M.P., Cooke, P.J., Nelson, C.S., Spiegler, D., 2005. Intraspecific morphological variation in late Miocene Bolboforma, and implications for their classification, ecology, and biostratigraphic utility. Mar. Micropaleontol. 56, 161–176.

Davies, P.J., McKenzie, J.A., Palmer-Julson, A., et al., 1991. Proc. Ocean Drill. Proj., Init. Repts, p. 133.

Davies, P.J., Symonds, P.A., Feary, D.A., Pigram, C.J., 1989. The evolution of the carbonate platforms of Northeast Australia. Soc. econ. Paleont. Mineral., Spec. Publ. 44, 233–258.

de Vos, A., Pattiaratchi, C.B., Wijeratne, E.M.S., 2014. Surface circulation and upwelling patterns around Sri Lanka. Biogeosciences 11, 5909–5930.

DiCaprio, L., Müller, R.D., Gurnis, M., 2010. A dynamic process for drowning carbonate reefs on the northeastern Australian margin. Geology 38, 11–14.

Droxler, A.W., Haddad, G.A., Kroon, D., Gartner, S., Wei, W., McNeill, D., 1993. Late Pliocene (2.9 Ma) partial recovery of shallow carbonate banks on the Queensland

Plateau: Signal of bank-top reentry into the photic zone during a lowering in sea level. Proc. Ocean Drill. Proj. Sci. Results 133, 235–254.
Eberli, G.P., Anselmetti, F.S., Isern, A.R., Delius, H., 2010. Timing of changes in sea level and currents along Miocene platforms on the Marion Plateau. In: Morgan, W.A., George, A.D., Harris, P.M., Kupecz, J.A., Sarg, J.F. (Eds.), Cenozoic carbonate systems of Australasia, pp. 219–242.
Elmer, F., Rogers, J.S., Dunbar, R.B., Monismith, S.G., Bell, J.J., Gardner, P.A., 2016. Influence of localised currents, benthic community cover and composition on coral recruitment: integrating field-based observations and physical oceanographic modelling. In: Proceedings of the 13th International Coral Reef Symposium, Honolulu, pp. 101–142.
Feary, D.A., Champion, D.C., Bultitude, R.J., Williams, A., 1993. Igneous and metasedimentary basement lithofacies of the Queensland Plateau (Sites 824 and 825). Proc. Ocean Drill. Proj. Sci. Results 133, 535–540.
Flower, B.P., Kennett, J.P., 1994. The middle Miocene climatic transition: East Antarctic ice sheet development, deep ocean circulation and global carbon cycling. Palaeogeogr. Palaeoclimatol. Palaeoecol. 108, 537–555.
Gartner, S., Wei, W., Kroon, D., Betzler, C., 1993. Intercalibration of Leg 133 biostratigraphies. Proc. Ocean Drill. Proj. Sci. Results 133, 697–704.
Glenn, C.R., Kronen Jr., J.D., 1993. Origin and significance of late Pliocene Phosphatic Hardgrounds on the Queensland Plateau, Northeastern Australian Margin. Proc. Ocean Drill. Proj. Sci. Results 133, 525–534.
Groeneveld, J., Henderiks, J., Renema, W., McHugh, C.M., De Vleeschouwer, D., Christensen, B.A., Fulthorpe, C.S., Reuning, L., Gallagher, S.J., Bogus, K., Auer, G., Ishiwa, T., 2017. Australian shelf sediments reveal shifts in Miocene Southern Hemisphere westerlies. Sci. Adv. 3 https://doi.org/10.1126/sciadv.1602567.
Hallock, P., Schlager, W., 1986. Nutrient excess and the demise of coral reefs and carbonate platform. Palaios 1, 389–398.
Haq, B.U., Hardenbol, J., Vail, P.R., 1988. Mesozoic and Cenozoic chronostratigraphy and cycles of sea-level change. Soc. econ. Paleont. Mineral Spec. Publ. 42, 71–108.
Harii, S., Kayanne, H., 2002. Larval Settlement of Corals in Flowing Water using a Racetrack Flume. Mar. Technol. Soc. J. 36, 76–79.
Hata, T., Madin, J.S., Cumbo, V.R., Denny, M., Figueiredo, J., Harii, S., Thomas, C.J., Baird, A.H., 2017. Coral larvae are poor swimmers and require fine-scale reef structure to settle. Sci. Rep. 7, 2249. https://doi.org/10.1038/s41598-017-02402-y.
Hays, J.D., Imbrie, J., Shackleton, N.J., 1976. Variations in the earth's orbit: pacemaker of the ice ages. Science 194, 1121–1132.
Heron, S.F., Maynard, J.A., van Hooidonk, R., Eakin, C.M., 2016. Warming Trends and Bleaching stress of the World's Coral Reefs 1985–2012. Sci. Rep. 6, 38402.
Holbourn, A., Kuhnt, W., Clemens, S., Prell, W., Andersen, N., 2013. Middle to late Miocene stepwise climate cooling: evidence from a high-resolution deep water isotope curve spanning 8 million years. Paleoceanography 28, 688–699.
Isern, A., Anselmetti, F.S., Blum, P., 2004. A Neogene carbonate platform, slope and shelf edifice shaped by sea level and ocean currents, Marion Plateau (Northeast Australia). In: Eberli, G.P., Masaferro, J.L., Sarg, J.F. (Eds.), Seismic imaging of carbonate reservoirs and systems., 291-307.
Isern, A., McKenzie, J.A., Feary, D.A., 1996. The role of sea-surface temperature as a control on carbonate platform development in the western Coral Sea. Palaeogeogr. Palaeoclimatol. Palaeoecol. 124, 247–272.
Isern, A., McKenzie, J.A., Müller, D.W., 1993. Paleoceanographic changes and reef growth off the Northeastern Australian margin: Stable isotopic data from Leg 133, Sites 811 and 817, and Leg 21, Site 209. Proc. Ocean Drill. Proj. Sci. Results 133, 263–280.
James, N.P., 1997. The cool-water carbonate depositional realm. In: James, N.P., Clarke, J.A.D. (Eds.), Cool-water carbonates. Soc. econ. Paleont. Mineral Spec. Publ. 56, 1–20.
John, C.M., Mutti, M., 2005. Relative Control of Paleoceanography, climate, and Eustasy over Heterozoan Carbonates: a Perspective from Slope Sediments of the Marion Plateau (ODP LEG 194). J. Sediment. Res. 75, 216–230.
Katz, M.E., Miller, K.G., 1993. Neogene subsidence along the Northeastern Australian margin: Benthic foraminiferal evidence. Proc. Ocean Drill. Proj Sci. Results 133, 75–92.
Kessler, W.S., Cravatte, S., 2013. Mean circulation of the Coral Sea. J. Geophys. Res. Oceans 118, 6385–6410.
Laugié, M., Michel, J., Pohl, A., Poli, E., Borgomano, J., 2019. Global distribution of modern shallow-water marine carbonate factories: a spatial model based on environmental parameters. Sci. Rep. 9, 16432. https://doi.org/10.1038/s41598-019-52821-2.
Ling, A., Eberli, G.P., Swart, P.K., Reolid, J., Stainbank, S., Rüggeberg, A., Betzler, C., 2021. Middle Miocene platform drowning in the Maldives associated with monsoon-related intensification of currents. Palaeogeogr. Palaeoclimatol. Palaeoecol. 567, 110275 https://doi.org/10.1016/j.palaeo.2021.110275.
Lisiecki, L.E., Raymo, M.E., 2005. A Pliocene-Pleistocene stack of 57 globally distributed benthic D18O records. Paleoceanography 20. https://doi.org/10.1029/2004PA001071. PA 1003.
McNeill, D.F., Guyomard, T.S., Hawthorne, T.B., 1993. Magnetostratigraphy and the nature of magnetic remanence in platform/periplatform carbonates, Queensland Plateau, Australia. Proc. Ocean Drill. Proj. Sci. Res. 133, 573–614.
Miller, K.G., Browning, J.V., Schmelz, W.J., Kopp, R.E., Mountain, G.S., Wright, J.D., 2020. Cenozoic Sea-level and cryospheric evolution from deep-sea geochemical and continental margin records. Sci. Adv. 6, eaaz1346 https://doi.org/10.1126/sciadv.aaz1346.
Müller, R.D., Lim, V.S.L., Isern, A.R., 2000. Late Tertiary tectonic subsidence on the northeast Australian passive margin: response to dynamic topography? Mar. Geol. 162, 337–352.
Mullins, H.T., Neumann, A.C., Wilber, R.J., Hine, A.C., Chinburg, S.J., 1980. Carbonate sediment drifts in Northern Straits of Florida. Am. Assoc. Pet. Geol. Bull. 64, 1701–1717.
Mutter, J.C., 1977. The Queensland Plateau. Bur. Min. Resour., Geol. Geophys., Bull. 179, 1–55.
Orme, G.R., 1977. The Coral Sea Plateau - a major reef province. In: Jones, O.A., Endean, R. (Eds.), Biology and Geology of Coral Reefs. Academic Press, New York, pp. 267–306.
Petrick, B., Reuning, L., Auer, G., Zhang, Y., Pfeiffer, M., Schwark, L., 2023. Warm, not cold temperatures contributed to a late Miocene reef decline in the Coral Sea. Sci. Rep. 13, 4015. https://doi.org/10.1038/s41598-023-31034-8.
Raffi, I., Wade, B.S., Pälike, H., Beu, A.G., Cooper, R., Crundwell, M.P., Krijgsman, W., Moore, T., Raine, I., Sardella, R., Vernyhorova, Y.V., 2020. Chapter 29 - the Neogene Period. In: Gradstein, F.M., Ogg, J.G., Schmitz, M.D., Ogg, G.M. (Eds.), Geologic Time Scale 2020. Elsevier, pp. 1141–1215.
Rankey, E.C., 2020. Eustatic, Climatic, and Oceanographic Influences on Geomorphology and Architecture of Isolated Carbonate Platforms: Miocene, Northwest Shelf, Australia. Lithosphere 2020, 8844754. https://doi.org/10.2113/2020/8844754.
Reolid, J., Betzler, C., Braga, J.C., Lüdmann, T., Ling, A., Eberli, G.P., 2020. Facies and geometry of drowning steps in a Miocene carbonate platform (Maldives). Palaeogeogr. Palaeoclimatol. Palaeoecol. 538, 109455 https://doi.org/10.1016/j.palaeo.2019.109455.
Roycroft, E., Fabre, P.H., MacDonald, A.J., Moritz, C., Moussalli, A., Rowe, K.C., 2022. New Guinea uplift opens ecological opportunity across a continent. Curr. Biol. 32, 4215–4224.
Schlager, W., 2003. Benthic carbonate factories of the Phanerozoic. Int. J. Earth Sci. 92, 445–464.
Schlager, W., 2005. Carbonate sedimentology and sequence stratigraphy. Concepts Sediment. Paleont. 8, 200 pp.
Siwabessy, J., Spinoccia, M., 2022. Processed EM710 Acoustic Backscatter, Sidescan and Swath Bathymetry Data acquired during R/V Falkor expedition FK200802 (2020). IEDA. https://doi.org/10.26022/IEDA/330880.
Storlazzi, C.D., Elias, E., Field, M.E., Presto, M.K., 2011. Numerical modeling of the impact of sea-level rise on fringing coral reef hydrodynamics and sediment transport. Coral Reefs 30, 83–96.
Sugden, D.E., Marchant, D.R., Denton, G.H., 1993. The Case for a Stable East Antarctic Ice Sheet: the Background. Geografiska Annaler Series A, Physical Geography 75, 151–154.
Taylor, L., Falvey, D., 1977. Queensland Plateau and Coral Sea Basin: Stratigraphy, structure and tectonics. Austral. Petrol. Explor. Assoc. Jour. 17, 13–29.
Thronberens, S., Back, S., Bourget, J., Allan, T., Reuning, L., 2022. 3D seismic-chronostratigraphy of reefs and drifts in the Browse Basin, NW Australia. GSA Bull. 134, 3155–3175.
van Hinsbergen, D.J.J., de Groot, L.V., van Schaik, S.J., Spakman, W., Bijl, P.K., Sluijs, A., Langereis, C.G., Brinkhuis, H., 2015. A Paleolatitude Calculator for Paleoclimate Studies. PLoS One 10. https://doi.org/10.1371/journal.pone.0126946.
van Ufford, A.Q., Cloos, M., 2005. Cenozoic tectonics of New Guinea. AAPG Bull. 89, 119–140.
Wunsch, M., Betzler, C., Eberli, G.P., Lindhorst, S., Lüdmann, T., Reijmer, J.J.G., 2018. Sedimentary dynamics and high-frequency sequence stratigraphy of the southwestern slope of Great Bahama Bank. Sediment. Geol. 363, 96–117.
Wyrtki, K., 1962. The Subsurface Water Masses in the Western South Pacific Ocean. Mar. Freshw. Res. 13, 18–47.
Zachos, J., Pagani, M., Sloan, L., Thomas, E., Billups, K., 2001. Trends, Rhythms, and Aberrations in Global climate 65 Ma to present. Science 292, 686–693.